Water-Soluble Fluorinated and PEGylated Cyanostilbene Derivative: An Amphiphilic Building Block Forming Self-Assembled Organic Nanorods with Enhanced Fluorescence Emission

Seunghoon Shin,[a,b] *Se Hoon Gihm*,[c] *Chong Rae Park*,[c] *Sehoon Kim*,[*,b] and *Soo Young Park*[*,a]

[a]*Center for Supramolecular Optoelectronic Materials, WCU Hybrid Materials Program, Department of Materials Science and Engineering, Seoul National University, Seoul 151-744, Korea. E-mail: parksy@snu.ac.kr.* [b]*Center for Theragnosis, Korea Institute of Science and Technology, 39-1 Hawolgok-dong, Seongbuk-gu, Seoul 136-791, Korea. E-mail: sehoonkim@kist.re.kr.* [c]*Carbon Nanomaterials Design Laboratory, Global Research Laboratory, Research Institute of Advanced Materials, and Department of Materials Science and Engineering, Seoul National University, Seoul 151-744, Korea.*

Supplementary Figures

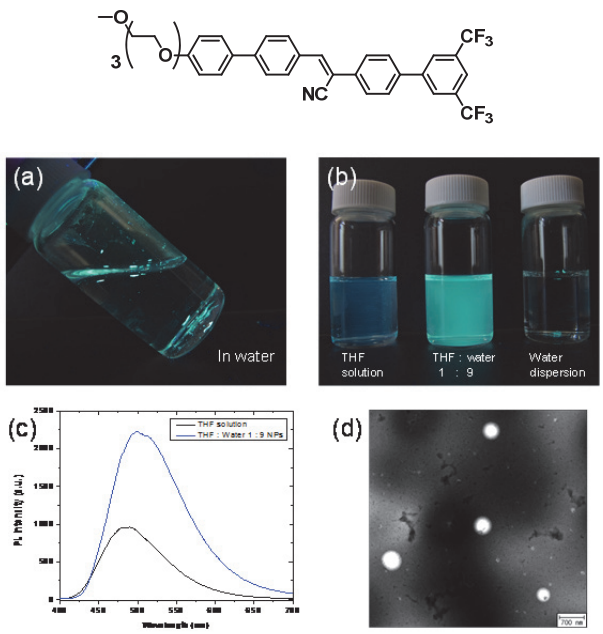

Figure S1. Chemical structure of 3EO-CNTFMBE (top) and (a) fluorescence image showing its insolubility

in water. (b) Fluorescence views of homogeneous solution in THF, nanoprecipitates in THF/water (=1/9 by vol.) mixture and insoluble chunk immersed in water. Fluorescence photos in (a, b) were taken under a 365-nm UV lamp. (c) Photoluminescence spectra showing aggregation-induced fluorescence enhancement of 3EO-CNTFMBE. (d) TEM image of nanoprecipitates in (b), showing spherical aggregates precipitated from a THF solution to water.

[Characterization of 3EO-CNTFMBE]

^{13}C NMR (400 MHz, $CDCl_3$, ppm) δ = 159.09, 143.18, 142.44, 142.14, 138.68, 135.23, 132.51, 132.38, 132.18, 131.76, 130.04, 128.15, 127.85, 127.00, 126.78, 124.66, 121.95, 117.98, 115.15, 109.79, 71.95, 70.89, 70.69, 70.59, 69.73, 67.58, 59.04.

^{1}H NMR (400 MHz, $CDCl_3$, ppm) δ = 7.99 (m, 4H), 7.90 (s, 1H), 7.83 (d, 2H, J = 8.4 Hz), 7.58-7.72 (m, 7H), 7.02 (d, 2H, J = 8.8 Hz), 4.19 (t, 2H, J = 4.8 Hz), 3.89 (t, 2H, J = 4.8 Hz), 3.55-3.78 (m, 8H), 3.39 (s, 3H).

Figure S2. Setup for GIXD experiments with a plate-like bulk solid of 12EO-CNTFMBE, showing the small incident angle for the incoming X-ray.

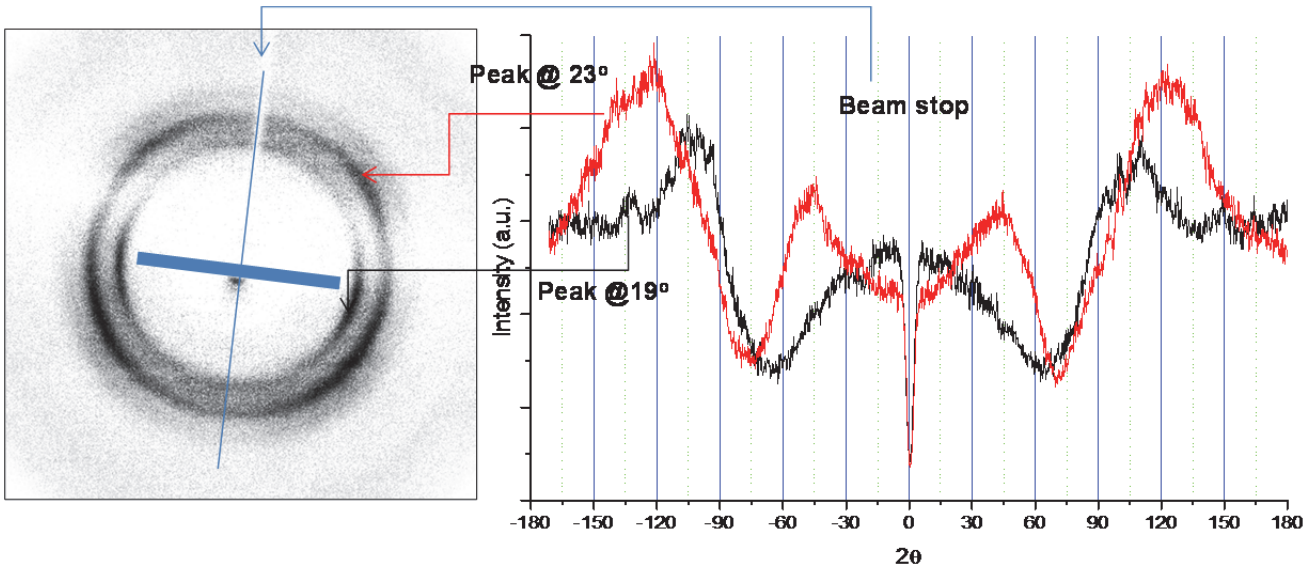

Figure S3. Azimuthal scan profile (right) for the wide-angle GIXD pattern (left) of 12EO-CNTFMBE bulk.

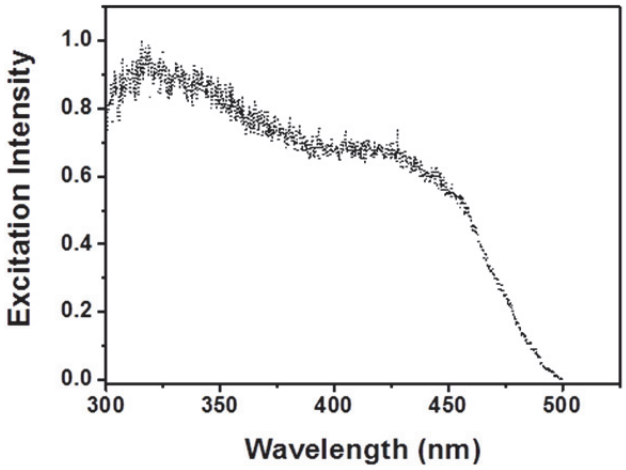

Figure S4. Photoluminescence excitation spectrum of 12EO-CNTFMBE bulk ($\lambda_{fl.}$= 530 nm).

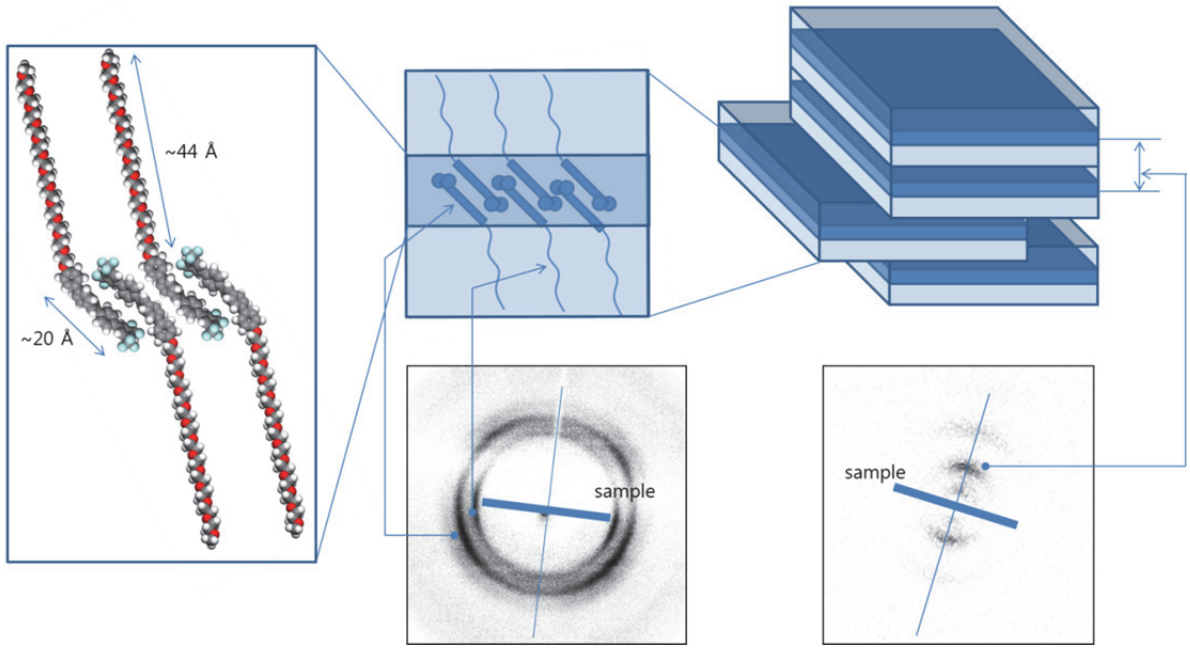

Figure S5. Schematic representation of the molecular arrangement model for 12EO-CNTFMBE in bulk, proposed on the basis of the GIXD results.

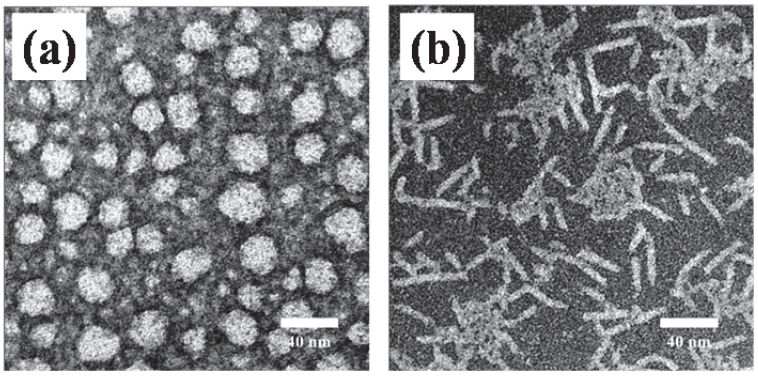

Figure S6. TEM images: (a) Nanoaggregates of Nile Red formed by sonication in water and (b) self-assembled nanorods of 12EO-CNTFMBE in water, doped with Nile Red (0.2 wt%).

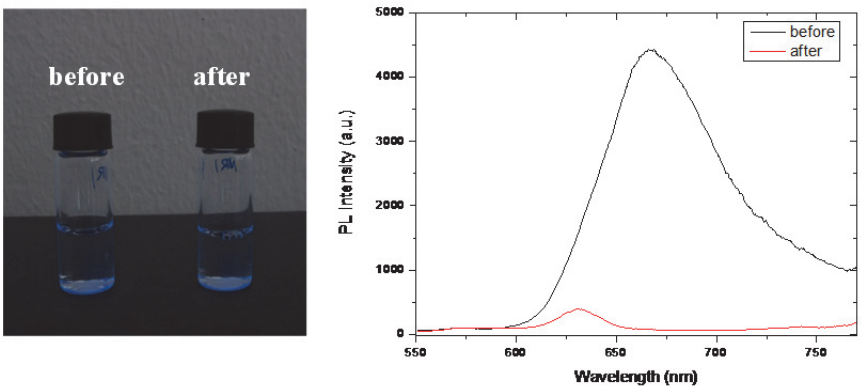

Figure S7. Fluorescence image and spectra of Nile Red self-aggregates before and after cross flow membrane filtration.

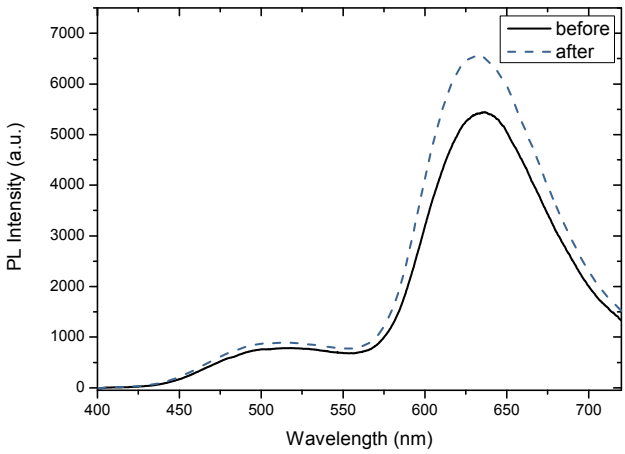

Figure S8. Fluorescence spectra of Nile Red-loaded 12EO-CNTFMBE nanorods before and after cross flow membrane filtration.

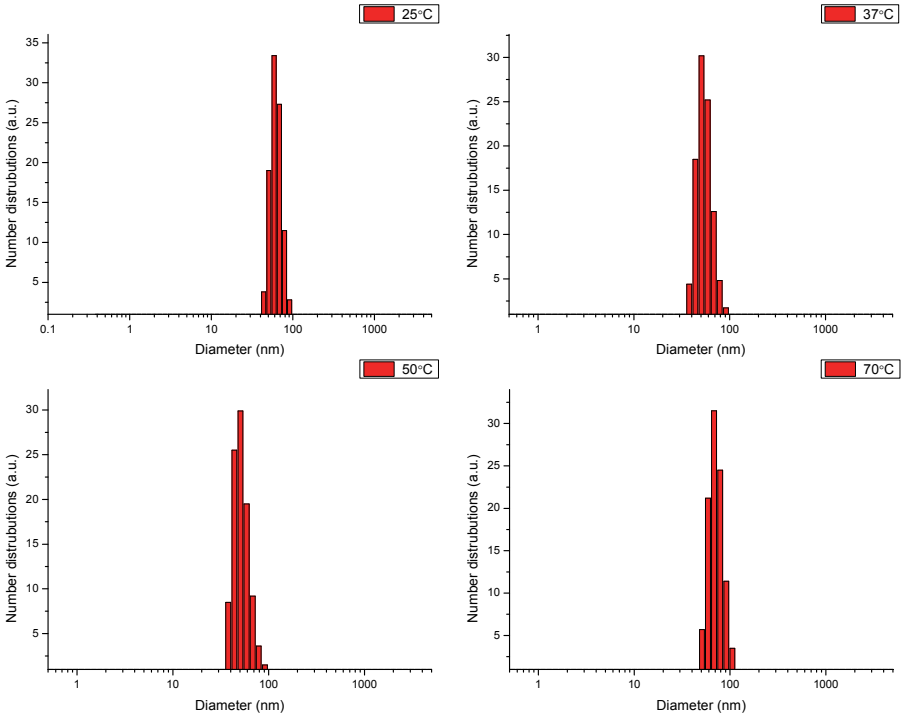

Figure S9. Temperature-dependent hydrodynamic sizes of the 12EO-CNTFMBE nanorods formed in water at 0.1 mg/mL, measured by dynamic light scattering (DLS; Nano-ZS, Malvern).

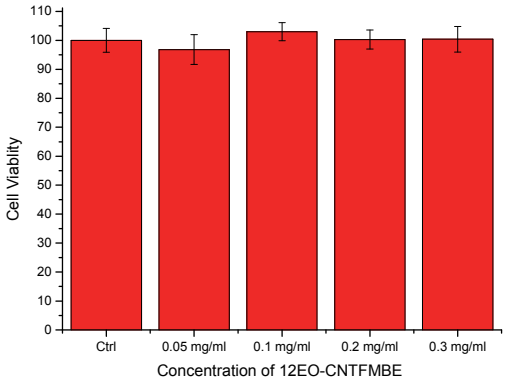

Figure S10. In vitro MTT assay showing cytotoxicity of 12EO-CNTFMBE nanorods against HeLa cells at varying concentrations. Cells were treated with samples for 3 h and then subjected to MTT assay.

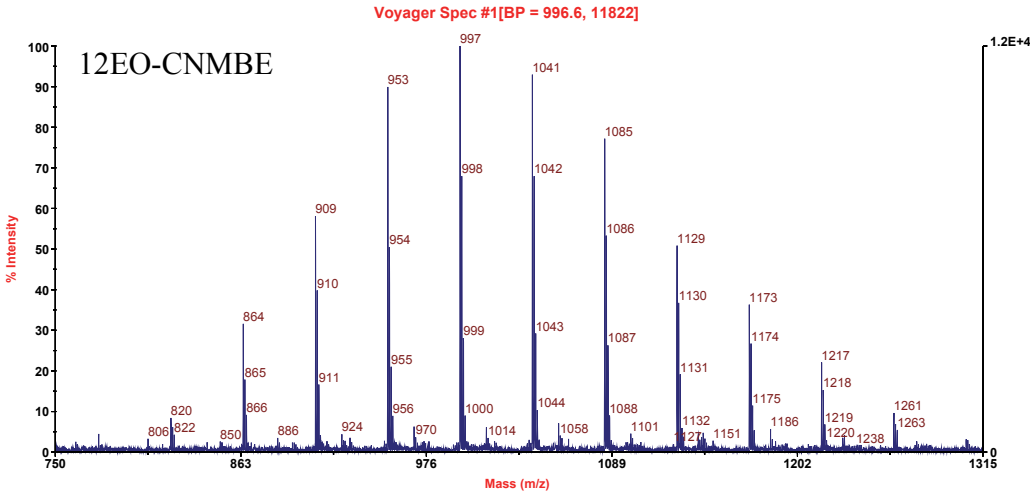

Calcd for $C_{55}H_{75}NO_{14}$, *m/z* = 996.51 ($M+Na^+$); found, 997 ($M+Na^+$).

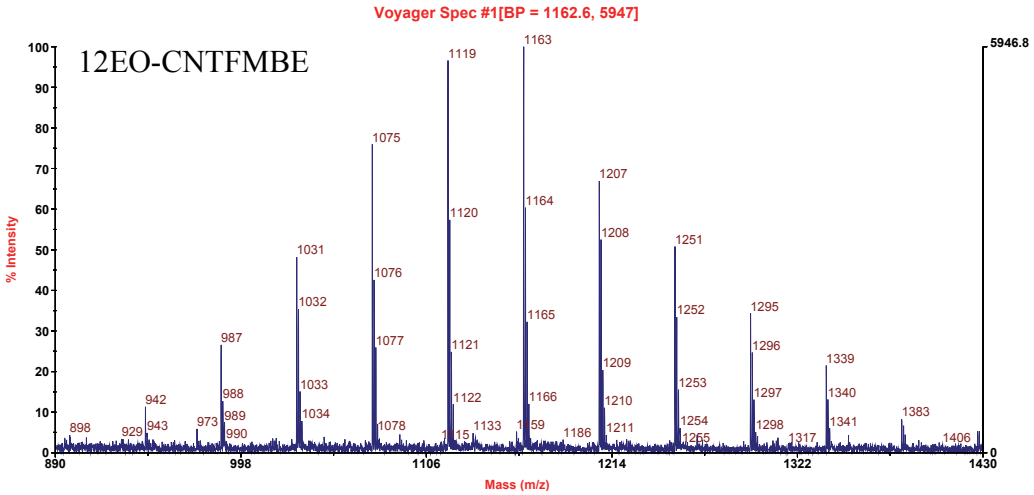

Calcd for $C_{56}H_{71}F_6NO_{14}$, *m/z* = 1119.14 ($M+Na^+$); found, 1119 ($M+Na^+$).

Figure S11. MALDI-TOF mass spectrometers of 12EO-CNMBE (upper) and 12EO-CNTFMBE (lower). Among mixture peaks arising from the polydispersity nature of polymeric PEG coil, the theoretical and found mass values for components having a PEG coil of $–O(CH_2CH_2O)_{12}CH_3$ are indicated.